Fuel 345 (2023) 128194

Contents lists available at ScienceDirect

Fuel

journal homepage: www.elsevier.com/locate/fuel

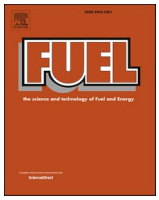

Full Length Article

Artificial neural networks for speeding-up the experimental calibration of propulsion systems

Luigi De Simio *, Sabato Iannaccone, Aniello Iazzetta, Maddalena Auriemma

Institute of Sciences and Technologies for Sustainable Energy and Mobility (STEMS), National Research Council, Via Marconi 4, 80125 Napoli, Italy

ARTICLE INFO

Keywords:
Artificial neural network training
Internal combustion engine optimization
Control map calibration
Multi-layer perceptron

ABSTRACT

Artificial neural networks have proven to be very useful, in different areas of investigation, for the realization of black box models able to represent the relationship between input and output data with high precision. In the automotive sector too, they have found widespread use, particularly for sub-models involving non-linear aspects. Most of these applications are not predictive, but mainly exploit the ability to obtain useful input–output relationships trough learning on scattered data. In contrast, the novelty of this paper is the use of a neural network, trained with experimental data in a portion of the operation area of the system to be calibrated, within a method used for forecasting purposes. The proposed framework consists of an iterative cycle of experimental tests, with control parameters identified by the neural network model, to reduce the time required for calibrating the entire working plan. This type of approach requires knowing the areas where the predictions of the model are sufficiently accurate. Therefore, a study was conducted for three different types of internal combustion engines, to evaluate a general trend of the prediction accuracy of the model, as a function of the distance from the training zone. In particular, the area where the learning was performed (10% of the engine operating plan) was expanded by 200%, with an error of approximately 5 times that of the training phase. Finally, the proposed method was compared with the best fitting surface approach and was found to be significantly reliable and accurate.

1. Introduction

Internal combustion engine (ICE) calibration has become more and more laborious, due to various supplementary strategy introduced in the last years to increase fuel conversion efficiency and decrease emissions. Among these, the most used are variable valve timing, downsizing, selective cylinder deactivation, or exhaust gas recycling. Hybrid vehicles further increase the complexity of calibration. Therefore, to avoid a considerable number of experimental tests, it would be necessary to adopt numerical models of the system under study. Complicated phenomenological models allow to make a digital twin; however, they must be sufficiently complete and accurate to be actually usable for calibration. In contrast, models based on artificial neural networks (ANN) are quite simple to implement and manage.

ANN has been largely proposed to build a virtual sensor for ICE. Gu et al. [1] mapped the instantaneous crank speed of an internal combustion engine versus in-cylinder pressure over the whole operating speed-load plane. The dataset was then used to train an ANN, which showed a reproducibility of data with a standard deviation on peak pressure, indicated mean effective pressure (IMEP) and maximum rate of pressure respectively of 9.3, 1.6 and 7.2%. A similar work has been conducted by Bizon et al. [2] but using as an input the vibration signal of an accelerometer mounted on the engine block of a three-cylinder diesel engine. Hoffmann et al. [3] proposed a virtual sensor through a multilayer perceptron network (MLP) controlling low -temperature combustion processes in ICEs. From intake valve closing and opening, injection parameters, and engine speed, evaluate combustion development. The calibrated model was then used as a closed-loop virtual combustion sensor.

ANNs were also proposed to build a simple black-box model of ICEs, thanks to the ability to describe non-linear links between the input and output variables of the model, better than other simple regression models can do. In [4], the authors compare four machine learning algorithms and a one-dimensional physical model to predict the exhaust gas temperature in a diesel engine converted to spark-ignition natural gas operation, using as inputs the spark timing, the equivalent ratio and the engine speed. They found that all of the machine learning models performed better than the physical one, with the artificial neural network algorithm being more accurate than the other three algorithms: random forest, support vector regression, and gradient increment regression trees. Che Wan et al. [5] compared the performance of an

* Corresponding author.
E-mail address: luigi.desimio@stems.cnr.it (L. De Simio).

https://doi.org/10.1016/j.fuel.2023.128194
Received 3 September 2022; Received in revised form 15 March 2023; Accepted 22 March 2023
Available online 28 March 2023

Nomenclature

Glossary

ANN	Artificial neural network
MAPE	Mean absolute percentage error
CI	Compression ignition
MIMO	Multi-input and multi-output
DOE	Design of experiments
MISO	Multi-input and single-output
ECU	Electronic control unit
MLP	Multi-layer perceptron network
G	Center of gravity
n	ICE speed
HD	Heavy duty
SA	Spark advance
ICE	Internal combustion engine
SI	Spark ignition
IMEP	Indicated mean effective pressure
SOI	Start of injection
LD	Light duty
THC	Total hydrocarbons
MAP	Manifold absolute pressure

ANN model with that of a mathematical model based on multiple regression techniques, that adopts the least square method approach. They found a mean absolute percentage error (MAPE) of ANN and the mathematical model between 1.9 and 9.3% and 4.1–28.3% respectively. Serikov [6] realized a mathematical model of an ICE with a feed -forward ANN and data in stationary conditions from the whole engine map. Different ANN layouts were tested and the one with 2 hidden layers and 8 neurons resulted the best to combine low complexity and good accuracy, showing a root-mean-square deviation of error on the training subset close to 3% for the modeled parameters. Mart [7] tested a 1.6-liter gasoline engine in transient conditions for deriving a data set to train a neural model for THC and CO evaluation, from engine speed, injection angle and fuel flow rate, showing good accuracy for transient maneuvers. Özener et al. [8] modeled a diesel engine with an ANN to predict the torque, power, brake-specific fuel consumption and pollutant emissions. About 100-test points were used: 50% for the training set, 30% for the test set, and 20% for the validation set, by a random selection. ANNs with one hidden layer and different numbers of neurons were tested, finding that the best estimation performance was in the range 5–16 neurons. Jahirul et al. [9] trained an ANN with a single hidden-layer architecture to predict the performance characteristics of a dual fuel multi-cylinder ICE. Engine load, speed and diesel-natural gas ratio have been used as the input layers, while engine thermal efficiency, break specific fuel consumption, exhaust temperature and air–fuel ratio have been used at the output layers. It was found that the optimal neuron number was in the range 6–8. A four-stroke diesel engine was modeled in [10] considering load, speed, fuel and airflow rates as the input parameters, while the outputs were brake power, mean effective pressure and volumetric efficiency. The data set of 1200 tests was divided into two parts as training (77%) and validation-testing (23%) sub-sets, with scattered data. The realized ANN showed mean error percentage values smaller than 1.15%. Similar results were obtained by Nwufo et al. [11] also for a single cylinder spark ignition engine fueled with ethanol–petrol blends, modeled at wide open throttle and variable engine speeds with an ANN of 10 neurons in hidden layers, to predict performance depending on the bioethanol mixture. In this case too, 70% of the experimental data set was used for training of the network, and the remaining 30% of the input data were used to test and validate the performance of the trained network. Uslu et al. [12] run a single-cylinder diesel engine with diethyl ether-diesel fuel mixtures at different blend ratios. Using 75% of the experimental results for training an ANN model, a mean relative error ranging from 0.5% to 4.8% was achieved. Liu et al. [13] used experimental data on a spark ignition engine to realize an ANN model. The dataset was randomly split: 66% for training and 34% to test the performance of the network. The mean relative error of the prediction ranged from 0.2% to almost 10%. A more extensive review of the application of an ANN in engine performance and exhaust emission characteristics was due by Yusri et al. [14].

Both for the multi-input single-output and for the multi-output topology in the works mentioned, the whole dataset is randomly partitioned with respect to training, testing and/or validation respectively, even if with different ratios. Many papers suggest of using ANN as ICE-black box model. However, if data are available in all operation ranges of the engine to be modeled, other black box models with spatial interpolation methods could be used, particularly to describe the engine parameters control map, predicting control values in unknown areas in an attempt to create a continuous surface from grid data points. The problem is very similar to the prediction of height for different point distributions on a digital elevation model. About this last aspect, Gumus et al. [15] performed a study aimed to quantify the effects of topographic variability and sampling density. In particular, errors of different interpolations (such as triangulation, or distance weighted) and ANN predictions were evaluated for different point distributions, finding that ANN is less effective in describing surface, if all data are considered in the training, because it deleted surface details and provided a smooth trend. Therefore, ANN could not be the best solution for engine control map issues.

Unlike most of the paper in the literature, the novelty of the present work is to demonstrate the feasibility of using a neural network to predict the optimal parameters outside the training zone in a reduced barycentric area of the propulsion system operating plan, which are then used to train an appropriate ANN. Even in the broad overview presented by Turkson et al. [16], or in the most recent state of the art review of Bhatt et al. [20], there are no references to papers using a method like the one presented in this study. The calculated parameter set can be considered a first attempt to conduct experimentation aimed at confirmation and refinement, speeding up the process of calibrating the powertrain control maps. Therefore, the study evaluates the possibility of using a neural network in a way that goes beyond that guaranteed by the “Universal Approximation Theorem for Neural Networks”, based on the proofs provided by Cybenko [17] for which there is certainly an ANN, with appropriate architecture, such as to describe any function in an approximate manner, for any number of inputs and outputs. Finally, the predictive ability of the developed ANN was investigated for three different thermal engines. The advantage of such a method would be relevant, especially for hybrid propulsion systems, in which more control parameters are required.

2. Aim of the study and procedures

In this study, the possibility of using neural networks in a procedure for calibrating control maps of internal combustion engines has been investigated. The procedure, described in the flowchart of Fig. 1, uses an MLP model for data forecasting. An MLP consists of at least an input layer, a hidden layer, and an output layer. The nodes of the hidden and output layers use a non-linear activation function to realize a non-linear mapping between inputs and output.

Generically, a propulsion system (the engines in this study) can be characterized by some parameters that identify the operating point, for example, speed and load, and others that specify how the system is maintained in those conditions (control parameters) and the performance (efficiency, emissions, etc.). Assuming the more general case in which the system has not been experimentally tested, or is under development, the range of variation (maximum and minimum values) of all these parameters can be established using different methods, such as estimates or by analyzing the datasheet of the different components, or

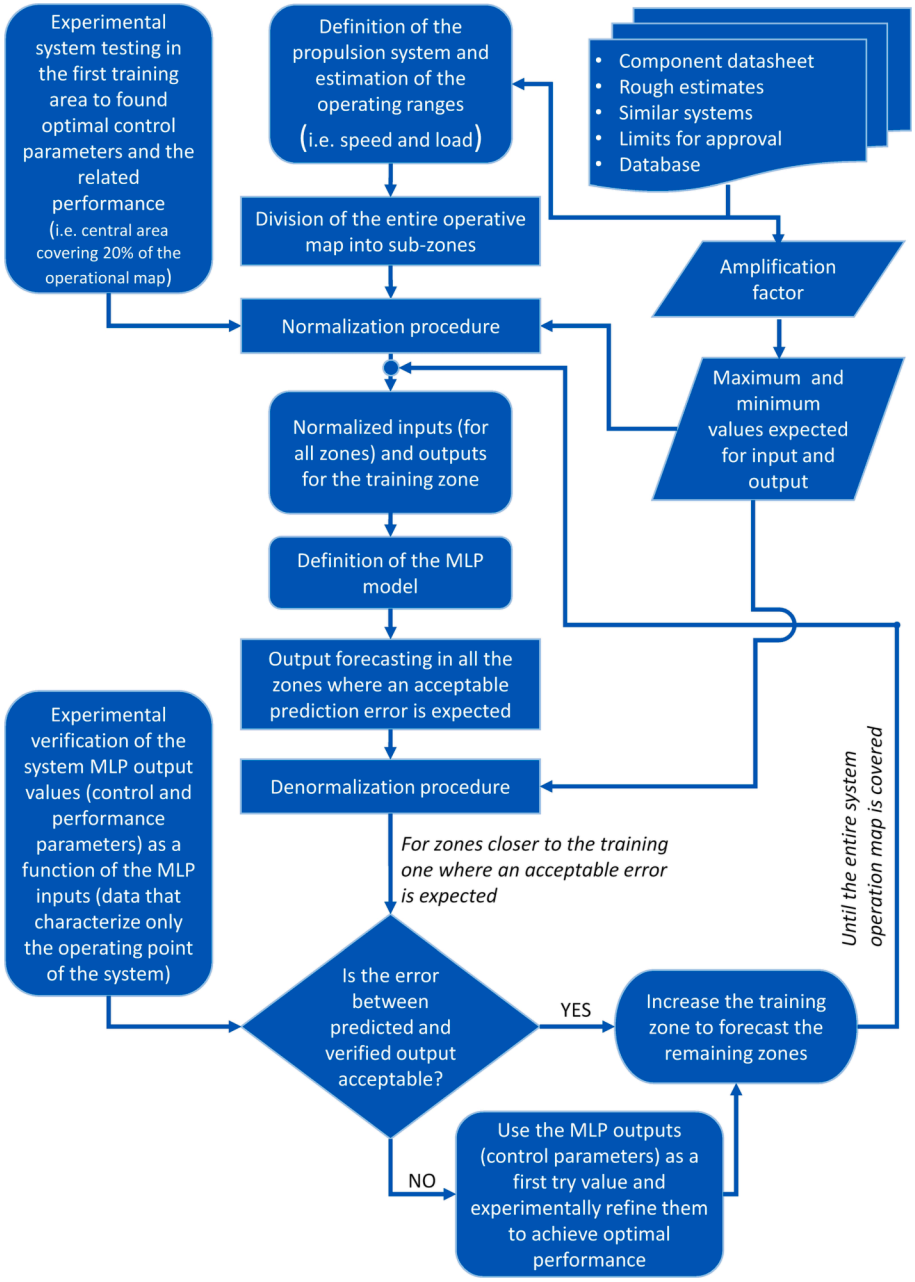

Fig. 1. Flowchart of the proposed framework to reduce experimental testing, in which the MLP model is integrated.

even setting limits on the expected performance. Therefore, an appropriate amplification factor could be set to expand the estimated ranges and cover some indeterminations. The set of all working points represents the operational map of the system, which can be divided into sub-zones. The first step of the proposed framework is to choose a sub-zone, reduced compared to the complete plan (i.e., a central area covering 20% of the operational map), in which the system is optimized with a specific design of experiments (DOE). The defined parameters with the estimated ranges, and experimental data, that can be used as training values, are therefore implemented in an MLP model. The maximum and minimum values of the ranges can be used for the normalization and denormalization procedure. The definition of the MLP model allows the forecasting of the outputs beyond the training zone. If, in the zones closer to the training area, the error between the predicted and experimentally verified outputs is acceptable, the cycle of calculation starts again from the updating of the training zone, and the re-evaluation of the outputs of the MLP model in the remaining zones, until the entire map is covered. In contrast, if the error is larger than the admissible, the MLP outputs, that means the engine control parameters, are used for their experimental refinement for optimal performance. At this stage, as in the previous case when the error was acceptable, the training zone is increased and the cycle of calculation starts again from the updated learning zone. The numerical part of the proposed framework can be considered free of limits for computational efforts, being simple both for the definition and the running phases. Surely, the limit lies in the experimental part, which requires more time, so it is useless to verify the forecasts in areas where a high error is already expected, but it is better to update the training area (with new experimental data obtained during the verification phase) and repeat the calculation run, to obtain a new more accurate forecast. The application of the procedure requires knowing the trend of the error of the MLP model as a function of the distance from the training sub-zone. Indeed, by establishing an error threshold, it is possible to determine a priori in which of the forecasting sub-zones conduct the experimental verification, before updating the

training zone. To this end, the MLP model was tested with the data of three internal combustion engines (one spark ignition for light duty, one spark ignition for heavy duty and another compression ignition for light duty), evaluating its accuracy to predict both optimal control parameters and related performance. The data set is made of about 700 values, obtained by triangulating the experimental data of the three engines. The neural networks were defined and trained only through a part of the available data, that is to say, around 20% in a barycentric position with respect to the two-dimensional operating plan representing an engine control map. Finally, the accuracy of the network in predicting the control map of the engine in the remaining part of the operating plan, whose data were not known to the network, was then evaluated. In particular, an analysis was carried out as the distance from the network's center of training increased.

2.1. Experimental data and reference data set

The experimental data were obtained on three different reference ICEs: a spark-ignition (SI) and a compression-ignition (CI) for passenger vehicles (light duty, LD), and a spark-ignition heavy duty (HD), of the typical size for city buses. The main characteristics of the ICEs are shown in Table 1.

The reference dataset used for defining the neural network and for verifying its reliability, was obtained as described in the following. For each ICE, the data have been acquired and determined on the test bed under steady-state conditions, in 20 different speed-torque points scattered throughout the operating plan adopting the optimal control maps. To enlarge the dataset of the selected parameters, the experimental data were processed through an extrapolation algorithm by using a suitable triangulation (between the 20 experimental points) and a rectangular grid of about 700 speed-torque points. Among the different possible alternatives to interpolate the relatively small number of data, the triangulation that provided the most realistic and regular fuel consumption map was chosen for each of the three engines. To select the best triangulation, the contour lines of the engine fuel consumption were evaluated. The contours are discrete plane curves, so that each curve is composed of connected straight line segments, with each segment belonging to a single triangle of the triangulation. The best triangulation was the one that maximizes the convex angle of intersection between two consecutive segments of the engine consumption contour lines, to have a smoother profile. Obviously, the nodes of the triangles coincide with the experimental data, while the triangles must not intersect each other, to have a single extrapolated value. The extrapolation is then simply a matter of identifying the values (i.e., engine efficiency, engine-out emission, etc.) at each grid node (speed-torque points) within the right triangle. The same triangulation was then used to increase the dataset, both for fuel consumption values and for the other parameters used by the neural network. Therefore, the triangulation process only served to obtain a large number of data necessary for the machine learning process, starting from a limited number of experimental tests. The triangulation of experimental data was necessary for this study for both training and test areas for result validation. In the case of applying the method, triangulation would only be needed in the training area if the number of experimental data collected is not already large enough to feed the neural network.

Table 1
Main characteristics of engines.

Name	LD-SI	LD-CI	HD-SI
Type	Four-stroke SI	Four-stroke CI	Four-stroke SI
Fuel	Natural gas	Diesel oil	Natural gas
Number of cylinders	4	4	6
Displacement (cm^3)	1596	1910	7800
Valves/cylinder	2	2	4
Stroke (mm)	78	90.4	125
Bore (mm)	80.5	82	115
Compression ratio	10.5:1	18:1	11:1
Torque @ Nm/rpm	125 @ 4000	280 @ 2000	1100 @ 1100 ÷ 1650
Power @ kW/rpm	68 @ 5750	77 @ 5500	200 @ 2100

Fig. 2 shows the triangulation developed for the HD-SI engine. The numbers in the figure indicate the experimental test points therefore the torque and engine speed conditions for which all the measured parameters are available. The triangles identify the portions of the torque-speed plane used to interpolate the data. For each point belonging to a triangle, identified by a specific torque and engine speed conditions, it is possible to calculate a value of any engine performance using the experimental data of the same performance available at the vertices of the triangle. In this way, discretized elevation maps for each parameter can be constructed, which will consist of a set of triangular areas in the torque-speed-performance space. Figs. 3–5 show the trend of the fuel consumption elevation maps and the extrapolation grids of the dataset for all three engines. White circles identify the points at which the output data have been evaluated by the triangulation. All the extrapolated data, referring to a triangle that make up the triangulation, belong to a plane in space. Therefore, they are linked by a certain function to the corresponding abscissa and ordinates of the calculation grid. The entire data set, defined for different areas of the plane of the calculation grid, requires a high number of triangles, equal to about 30 for all three engines. This reason excludes the possibility that the neural network can easily predict the results, not being these all linked by a single mathematical function at the basis of the interpolation process. Furthermore, since the network will be trained on a central portion of the grid, only some of the generated triangles will be considered in the learning phase.

The data set obtained was subsequently divided into different regions, starting from the center of gravity (G) of the speed-load plane. The distances between each point and G were also evaluated and then normalized with respect to the maximum value. The ranges G-20%, 20–30%, 30–40%, 40–50%, 50–60%, 60–70%, 70–80% and 80–100% were used to set the analysis areas, as shown in Fig. 3b-5b for the three ICEs.

The MLP model was therefore defined with the aim of training the network only in the confined area G-20% of the ICE-optimized control parameters, and then predicting the optimal values outside the training area. The usefulness of this approach lies in the possibility of speeding up the calibration process, reducing the number of tests to be performed. Alternatively, it is required the use of complex numerical models or a long and expensive activity, with the help of DOE techniques, aimed at investigating the different possible combinations of the variables interested. The idea behind the proposed method is therefore to evaluate the

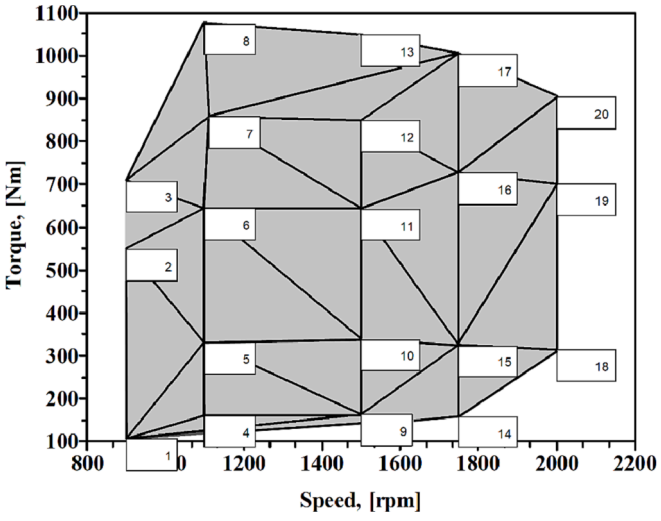

Fig. 2. Triangulation of the 20 experimental data available for the HD-SI engine.

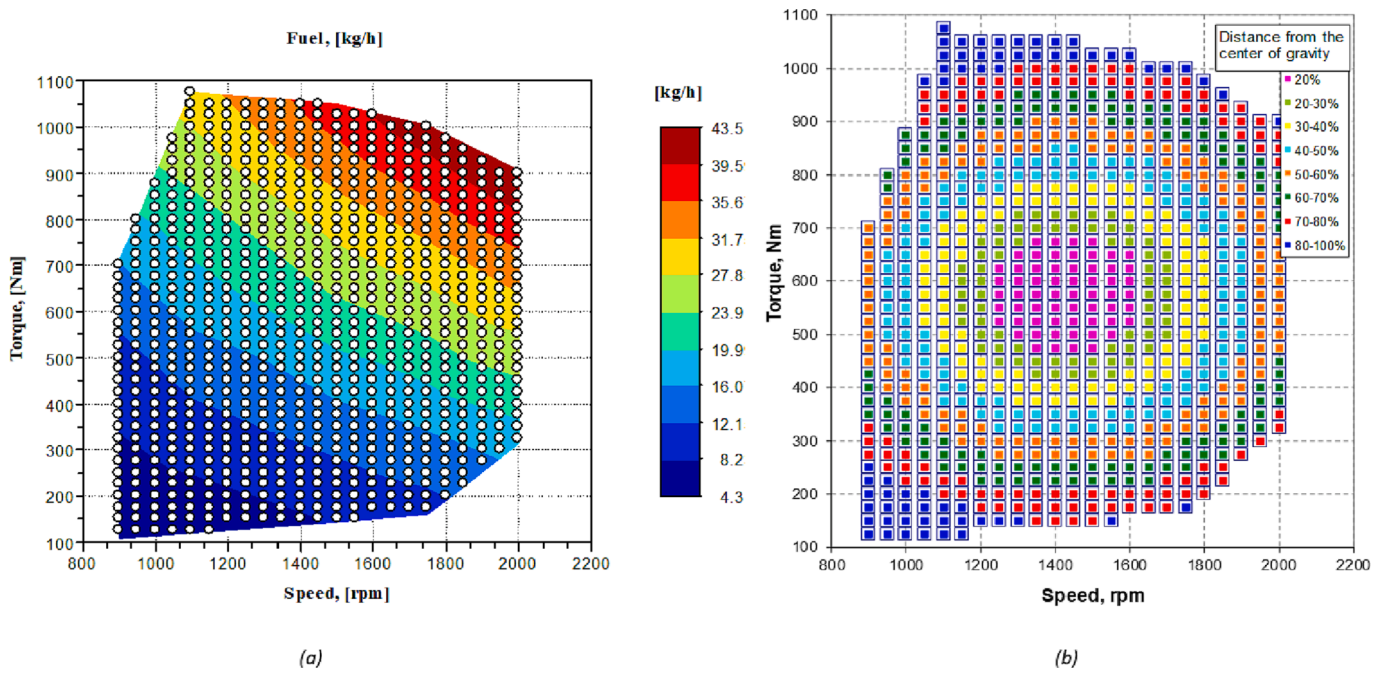

Fig. 3. Fuel consumption map and extrapolation grid of the dataset *(a)*, subdivision of the data in the different areas of distance from the center of gravity *(b)*, for the HD-SI engine.

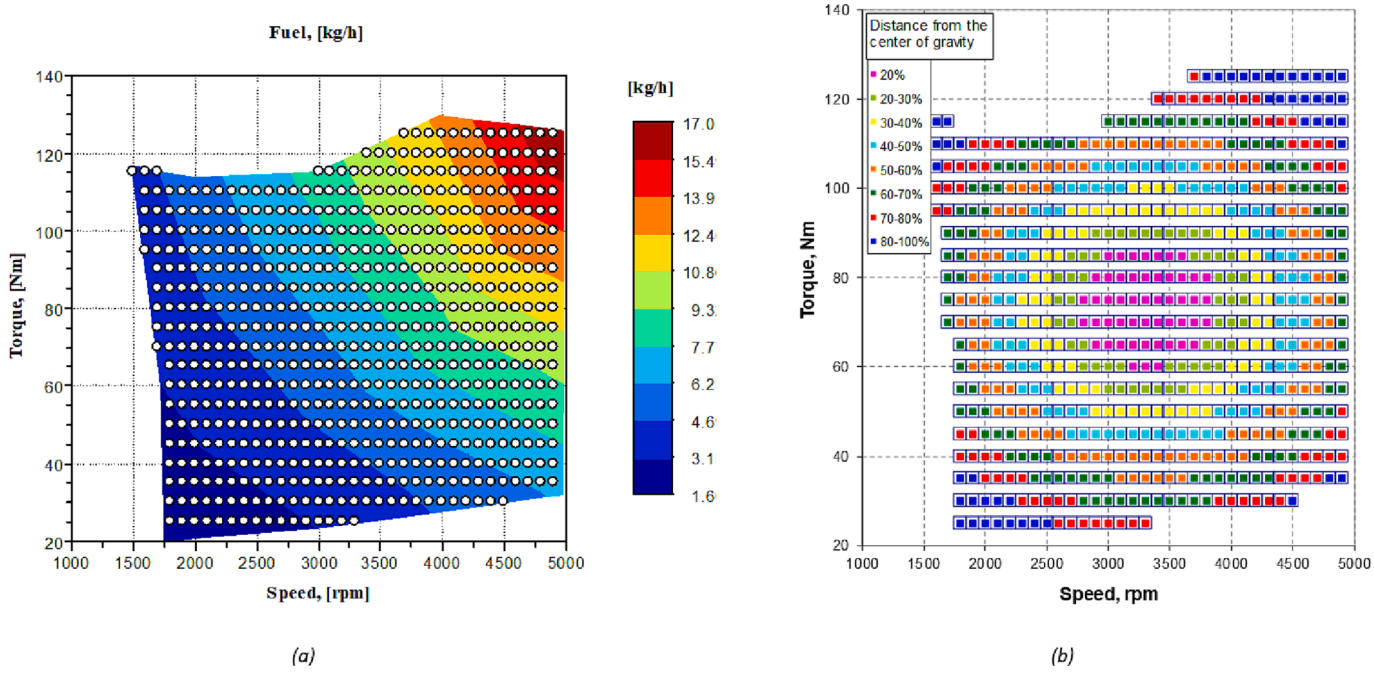

Fig. 4. Fuel consumption map and extrapolation grid of the dataset *(a)*, subdivision of the data in the different areas of distance from the center of gravity *(b)*, for the LD-SI engine.

accuracy of the MLP prediction, as the distance between the known and unknown regions increases.

2.2. Definition of network inputs/outputs

The objective of a network useful for the method schematized with the flowchart in Fig. 1 is to predict both the control parameters and the performance of a propulsion system outside the training area. The subsequent experimental verifications can then confirm the accuracy of the prediction or the need for refinement. In a propulsion system, the forward speed of the vehicle, proportional to the ICE speed, is the result of the driver's torque demand for each road load. The operating scheme of an electronic control unit (ECU) to govern this propulsion system is shown in Fig. 6, while the corresponding ANN scheme is shown in Fig. 7. Therefore, the ICE speed (n) and a control parameter related to the delivered torque have been chosen as network inputs. This parameter depends on the type of engine and the control strategies. For the SI engines has been selected the manifold absolute pressure (MAP), while for the CI engine, the most indicative parameter is the diesel fuel flow rate (FUEL). In the figures, the optimal parameters in blue refer to the SI

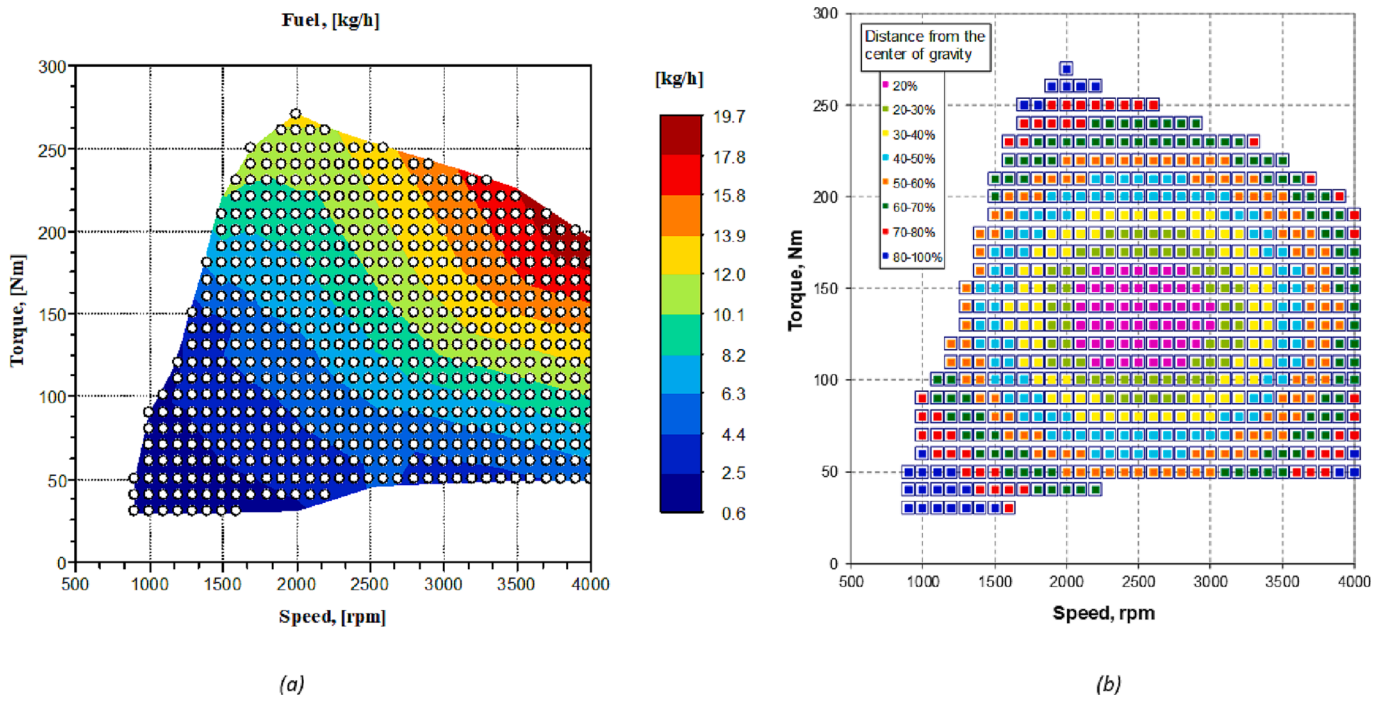

Fig. 5. Fuel consumption map and extrapolation grid of the dataset *(a)*, subdivision of the data in the different areas of distance from the center of gravity *(b)*, for the LD-CI engine.

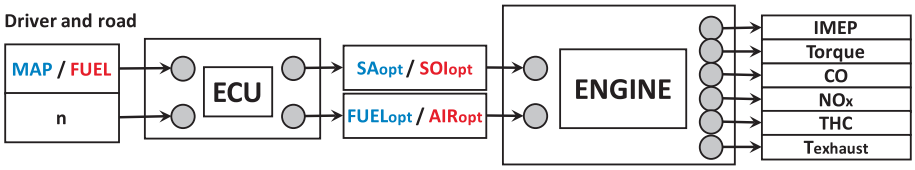

Fig. 6. Operating scheme of an engine with optimized control unit.

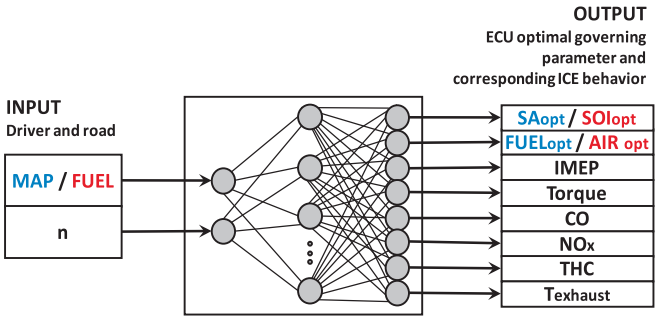

Fig. 7. ANN aimed at identifying optimal control parameters and engine performance based on the driver input and road conditions.

engine, while those in red to the CI engine. The network outputs are the optimal values of the control parameters with the associated engine performance. The formers set the operation of the engine in the zones outside the experimental optimization, where no data are available, while the latter characterize the engine behavior. All the output parameters of the network are necessary to verify the reliable of the predictions made by the model. Indeed, the experimental tests must confirm that, by setting the optimal parameters predicted by an ANN, engine performance resulted sufficiently close to those calculated. The selected output control parameters are: the fuel flow rate and the spark advance (SA), for the SI engines, and the airflow rate (AIR) and the start of injection (SOI), for the CI engine. The ECU establishes the governing parameters according to the load request and the response of the vehicle, given by the ICE speed. The quantities chosen to characterize the engine were: IMEP, related to the in-cylinder pressure cycle; torque, related to the engine volumetric efficiency; emissions, related to equivalent ratio and combustion conditions; and exhaust gas temperature, related to the wasted energy. From the selected input and output parameters of the ANN, most of the other data characterizing an engine behavior can be calculated, such as power and fuel conversion efficiency.

Otherwise, the case of a network set to model the engine in both optimized and non-optimized conditions would require a different approach. The operating scheme of the engine should be to that in Fig. 8. The corresponding ANN should have the ECU control parameters (SA and FUEL for SI engines and SOI and AIR for CI ones) as inputs together with those related to the driver and the road load, as shown in Fig. 9. Such a kind of network requires many experimental data to be trained and should be combined with a downstream optimization process for choosing the optimal values of the governing parameters. For example, the extension of the optimal results to a zone outside the training zone would require many simulations, varying the control parameters, and then the use of an optimization tool to find the best governing values. Instead, with the ANN of Fig. 7, this operation is easier, since optimal parameter values are directly an output of the network.

For the realization of the model, it was defined a single network with two inputs and eight outputs as shown in Fig. 7, configuring a multi-input and multi-output (MIMO) system, instead of eight networks with a single output (multi-input and single-output system, MISO), mainly because some initial tests showed that the error trend was not much

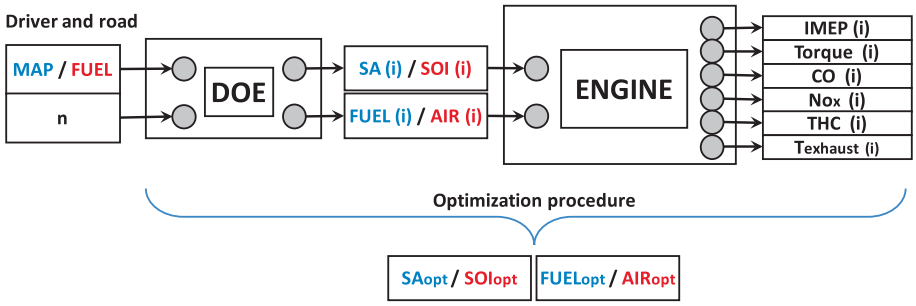

Fig. 8. Logical scheme of optimization of the control parameters through DOE.

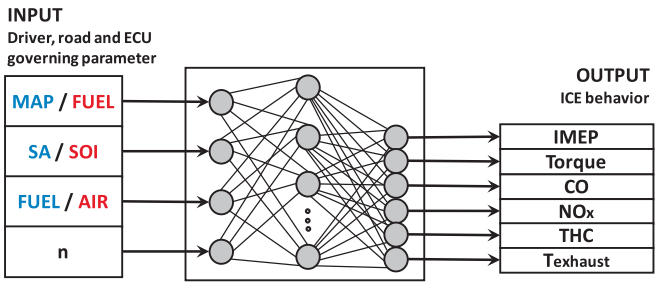

Fig. 9. ANN aimed at identifying engine performance based on driver input, road conditions and control parameters.

affected, whereas the management of eight different networks was more complicated.

Anyway, it must be mentioned that choice of MISO or MIMO system more appropriate may depend on the field of study. In the meteorological field for example, from a literature survey, it was found that most of the prediction models have been developed as MISO, although there are more convenient and efficient MIMO models [18]. Instead, in many practical cases more relevant to the energy field MIMO systems showed a greater capacity for predictions. For example, in the research by Pandey et al. [19] about energy from waste, additional tasks can improve the accuracy on the initial task, when there is a common description or, in other words, when the outputs are linked by the input condition. Moreover, the MIMO model may work better because of knowledge transfer from one output parameter to another. In particular, MIMO models were found to be more convenient than MISO, for internal combustion engines [20].

The proposed method has been validated with experimental data referring to engines equipped with original ECUs, optimized for approval according to specifications.

2.3. Definition of the neural network architecture

ANNs can be visualized as neurons interconnected that process information collectively, following the layer structure, from the input up to the output layer. This can happen through the hidden layers, which get information about the features of the problem by using weights. Each neuron can be regarded as a nonlinear transfer function from a multi-input to a single-output [21]. Weight values must be determined by training the network with a number of solved problems. In this paper, MLP artificial neural networks with a single hidden layer and binary encoding have been used. The training progress was managed by an evolutionary genetic algorithm, using both a crossover and a mutation operator to update the binary weight vector, until the optimal solution has been found. The mutation operator was designed as a co-mutation, to take care of the information shared between adjacent bits and among neighboring ones. In fact, in many cases, they are not completely independent one from another, rather they are encoded as a whole in the most general case of real variables [22].

To identify the number of neurons needed to describe the problem under examination, several analysis was carried out only with the LD-SI engine dataset, restricted to the G-20% area. The portion of data analyzed was randomly divided into a portion for network training (35 data) and a portion for network validation (16 data). The MAPE was then calculated on this second portion, with Eq. (1), where N is the number of samples:

$$MAPE = \frac{100}{N}\sum_{i=1}^{N}\frac{|output(i) - target(i)|}{target(i)} \quad (1)$$

In Fig. 10, the results of the analysis conducted by evaluating the MAPE of the one-dimensional output vector with respect to the one-dimensional target vector are shown. The two vectors were built considering all the 8 outputs and targets in the 16 points of the validation dataset, respectively, for a total value of N equal to 128. The inputs, the outputs, and the targets were normalized through the variation ranges, to allow the correlation of different quantities. The procedure is equivalent to the evaluation of the error for each individual network output and the calculation of the average value. The results show the need for a minimum number of neurons equal to 4, while it is useless to increase neurons beyond 8. Therefore, to choose a value for neurons, the predictivity of the network was evaluated, in terms of MAPE in all areas outside the training zone (G-20%), with 4, 7 and 10 neurons. Fig. 11 reports the result and indicates the seven-neuron network as the best of those considered, although qualitatively, the three networks do not differ much from each other. Global ranges, larger than that strictly necessary for the inputs and targets of the G-20% zone, were used for normalizing data, to allow the MLP of predicting values far from that used for the training zone. In particular, the range

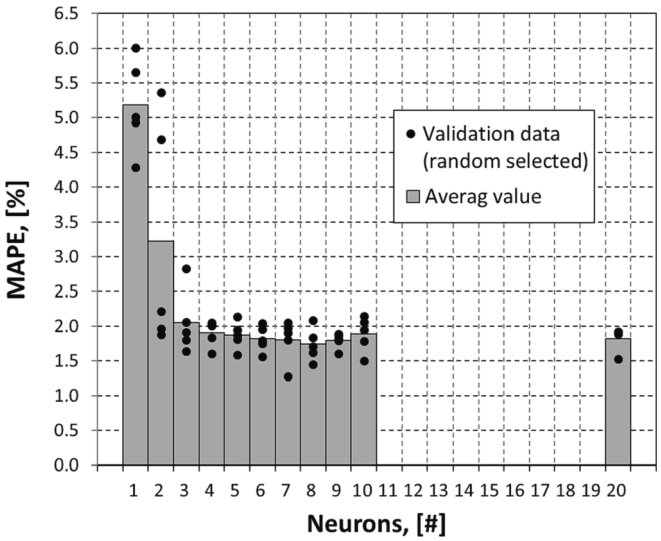

Fig. 10. MAPE trend with the number of neurons, for the LD-SI dataset.

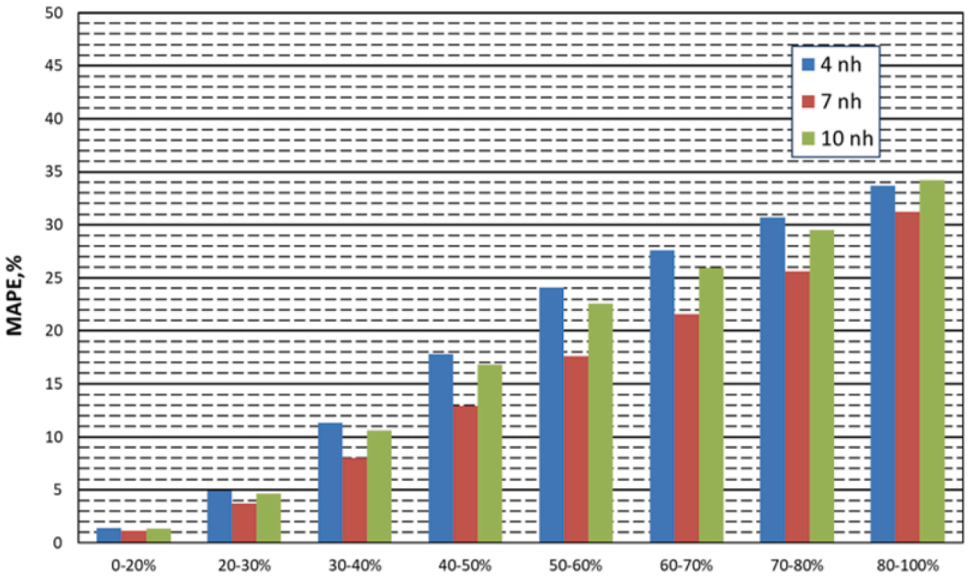

Fig. 11. MAPE trend with 4, 7 and 10 neurons, for the LD-SI dataset, in each subdivision zone.

(minimum–maximum) of the input and output data is obviously known in the case in question, however amplification factors of 1.2 and 0.8, respectively, for the maximum and the minimum values, were used, as if it were a general case. Moreover, the normalization range was set between −0.8 and 0.8, with Eq. (2) where *V* stands for *Value* and *NV* for *Normalized Value*, while *MIN* and *MAX* are the minimum and the maximum values of the expanded range. This last choice was made to allow the network to also foresee values outside the set ranges (i.e., normalized outputs ∈ [−1,−0.8] or [0.8, 1]) avoiding the problem of saturation of the outputs at the unit value for forecasts outside range.

$$NV = 1.6\frac{(V - MIN)}{(MAX - MIN)} - 0.8 \tag{2}$$

The type of transfer function for the neurons of the hidden layer and the output layer is a sigmoid represented by Eq. (3), where × denotes the scalar product between the matrix of the weights entering the hidden layer and the input vector, in the step from the input layer to the hidden layer, and between the matrix of the weights coming out of the hidden layer and the products of the first transfer function, in the passage from the hidden layer to the output.

$$f(x) = \frac{2}{1 + e^{(-2x)}} - 1 \tag{3}$$

The average data, expressed through the MAPE, have been assessed on all network output parameters, both those of control and those related to engine performance. The seven-neuron network indicates an average error of less than 10% in forecasting the data contained in the 20–30% and 30–40% ranges of the operation plan.

3. Results and discussion

The neural network with 7 neurons for the hidden layer and 1 bias for the input/output layers was used for the three available datasets, with calibration weights determined in the training phase, considering only the portion G-20% (0–20%) of the map of each engine. The same number of neurons was chosen even though seven neurons were found to be optimal for the LD-SI engine and may not be optimal for the other two engines. This choice was made because in the case of the application of the proposed method, the experimental data outside the training area would not be known, and it would not be possible to optimize the number of neurons by comparing the predictions with the target data. Therefore, for the other two engines, the number of neurons in the network was chosen according to the results of this study, as could be done in the case of the application of the proposed method. The average MAPE, evaluated on the total of the outputs, in comparison with the relative target is shown in Fig. 12. For the three engines, an error in the range 0.7–3% has been found in the G-20% region. In the regions where the network is used with the aim of predicting the optimal control parameters, as well as the consequent engine performance, appreciable differences emerge between the three engines, although the trends are similar. The error increases with the distance of the region from the training area, however the growing is greater for datasets with higher MAPE in the training phase. Therefore, it is important to perform this calibration process with very accurate experimental data, to obtain more approximate predictions. Nevertheless, there is another relevant aspect to consider. The forecast error, evaluated in relation to the training error, is much less dependent on the dataset, as shown in Fig. 13a, where the relationship between the MAPE in each subdivision of the operating plan and that of the training portion is reported. In Fig. 13b, the percentage of the covered operating plan as a function of the subdivisions is reported. Assuming MAPE training of 1%, it is possible to make predictions with an error less than 15% if the predicting zone is limited to the 65% range center subdivision (Fig. 13a). This range center corresponds to the 80% of the operating plan (Fig. 13b), while the training zone covered only the 10% of it. Therefore, predictions can be acceptable in area 700% wider than the training one. To obtain more accurate predictions, with a maximum MAPE of 5%, the acceptable forecasting area must be reduced from 700% to about 200% of the training area

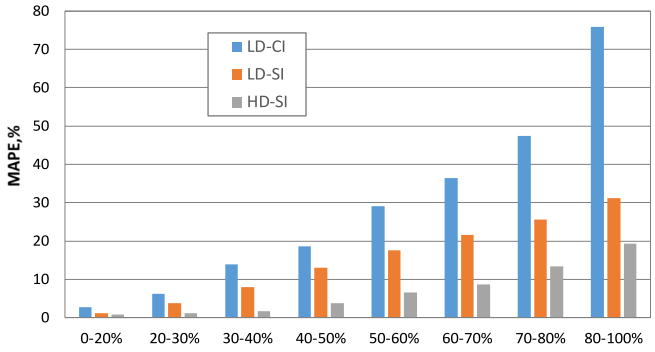

Fig. 12. MAPE trend with 7 neurons, for the three engine datasets, in each subdivision zone.

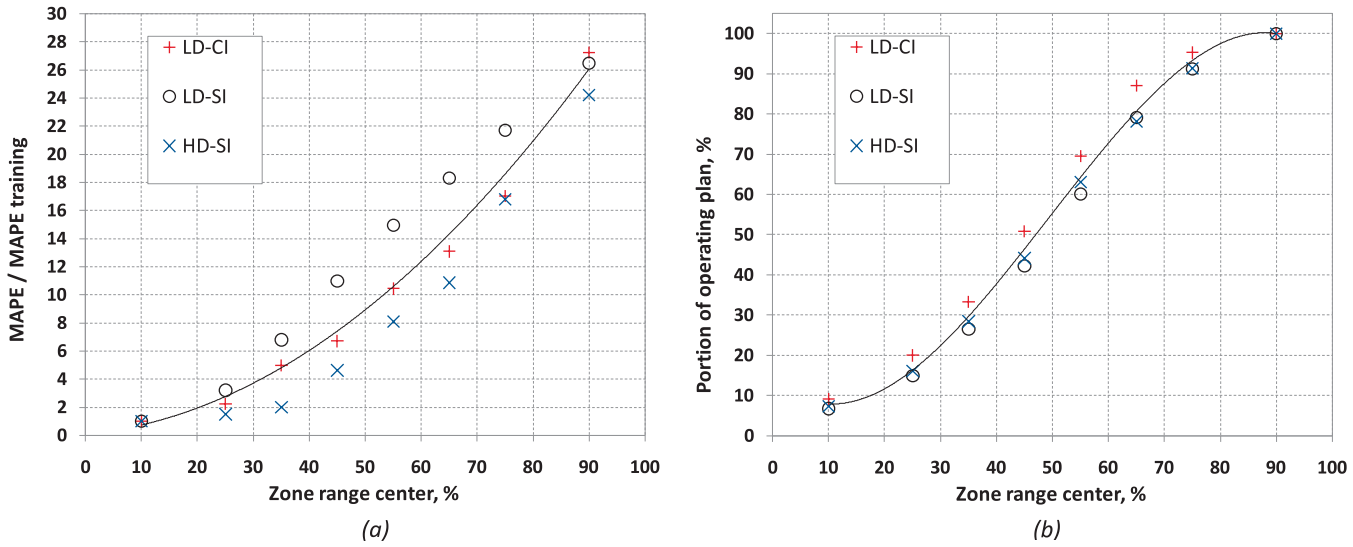

Fig. 13. For the three datasets: MAPE performance compared to MAPE training, (*a*), covered portion of the engine operating plan (*b*).

(roughly the zone with 35% range center).

In addition to the average values, the forecasts for the individual parameters calculated by the network were analyzed. With regard to the HD-SI case, Fig. 14 shows that the network, trained in sub-zone 0–20% with the speed between 1200 and 1700 rpm and MAP between 0.8 and 1.3 bar, must provide values in regions where the inputs are different up to 30–50%. In the LD-SI case, the network must provide values in areas with different input values up to 45% compared to those used for training, while the differences reach about 90% in the LD-CI case, for the input parameter linked to the fuel admission. Fig. 15 shows the comparison between the torque actually delivered by the engine (red symbols) and that expected from the network (black symbols). Although the torque falls far from the training set, the model predicts very well their maximum values actually delivered by all three engines. This behavior indicates that the network learns well the phenomenology that links the input parameters to the torque delivered by the engine in the training area and that this phenomenology does not change much in the forecast area. For the two SI engines, in addition to a good forecast quality, there is also a fair agreement with the experimental data, at least up to 60% of the operating plan. In the LD-CI case, however, the network forecast is much less precise, especially at medium loads. This is partly due to the greater training error, but also to the large difference in the values of the network inputs between the prediction zone and the training one.

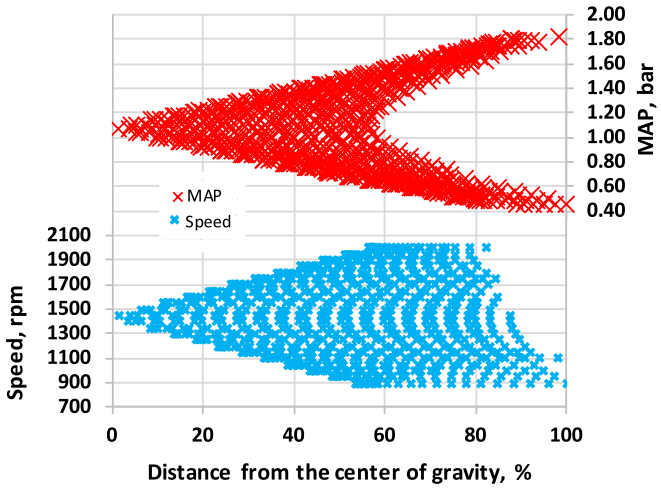

Fig. 14. Input data in training and forecasting zones for the HD-SI dataset.

Fig. 16 shows the comparison of THC emissions. At lower engine loads, where the target values are the highest, THC emissions are strongly underestimated by the model. This aspect resulted independent of the specific network under consideration. It could be due to a phenomenology irrelevant in the training area and therefore unable to influence the predictions of the model. A possible explanation may be that, at very part loads, the low operating temperature makes worse the combustion conditions, compared to those of the training area at a medium load, increasing unburnt products. For the same reason, the exhaust gas temperature drops at low loads, for all three engines, Fig. 17. In this case too, as this phenomenon is not predominant in the training area, the network forecasts differ markedly from the actual data. The circled target and output dots of Figs. 16 and 17 are for the lowest load conditions tested. For the naturally aspirated LD-SI engine, the circles highlight cases with MAP ranging from 0.4 to 0.5 bar, equal to approximately 20% of the total MAP range tested (0.4–1.0 bar). For the HD-SI turbo engine, circles highlight cases with MAP in the range 0.4–0.7 bar, equal to approximately 20% of the total MAP range tested on the engine (0.4–1.8 bar). Finally, for the compression ignition LD engine, circles highlight cases with FUEL in the range 0.5–4 kg/h, equal to about 20% of the total range of FUEL tested on the engine (0.5–20 kg/h). For the LD-CI engine, there are marked errors even under high load conditions, characterized by the high temperature of the exhaust gases in the areas furthest from the center of gravity. The cause is to be found in the marked difference in operating conditions between the training data and those in the more distant regions. A CI engine generally runs with a strong air excess at a medium load, which lowers the temperatures at the exhaust due to the dilution effect. This excess of air reduces at high load, where most of the available air is used to burn the fuel, with an increase in the temperatures at the exhaust. The net trained at medium loads cannot learn this different phenomenology linked to a minor excess of air.

On the other hand, the behavior of a propulsion system is optimized by means of different control strategies in the operating plan. For the three engines considered in this study, the strategies stored in the ECU work accordingly to the necessity of reducing engine-out emissions on the homologation cycle. These strategies also affect CO and NO_x besides THC emissions, by modifying parameters such as the combustion timing and the air–fuel ratio. Therefore, if the prediction of these parameters is affected of some imperfection, it can cause the increase in the average MAPE, especially moving away from the training area.

Fig. 18 shows the first predicted optimal governing parameter (output) related to the combustion timing SA, for the two SI engines, and

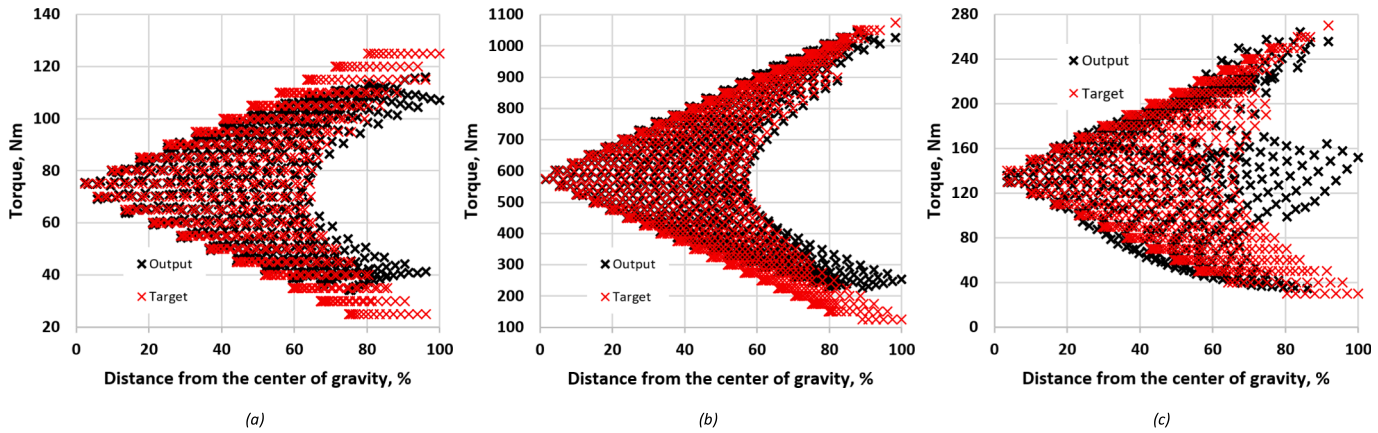

Fig. 15. Comparison between the target and expected torque for the three datasets: LD-SI *(a)*, HD-SI *(b)* and LD-CI *(c)*.

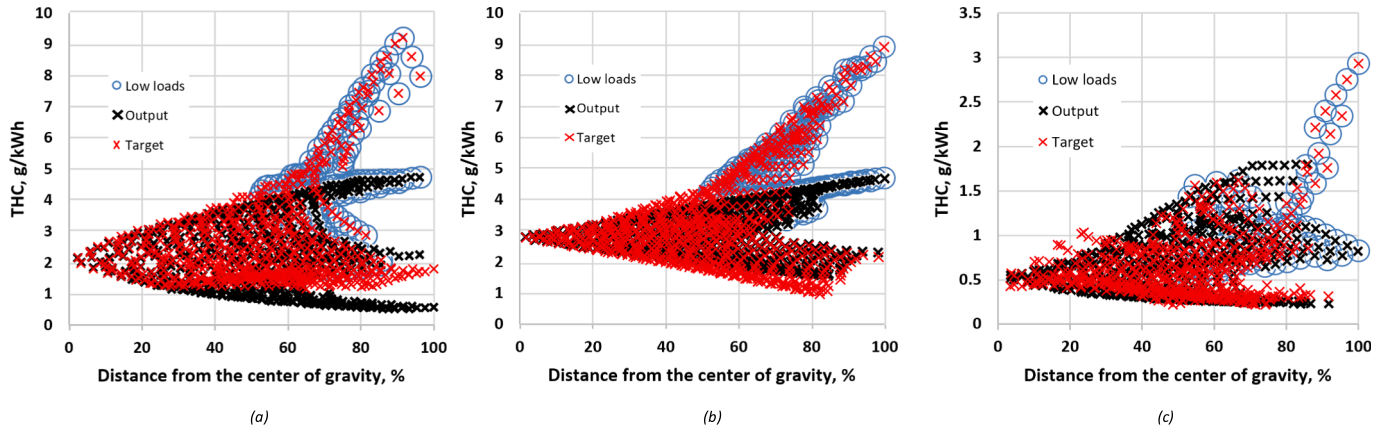

Fig. 16. Comparison between the target and expected THC for the three datasets: LD-SI *(a)*, HD-SI *(b)* and LD-CI *(c)*.

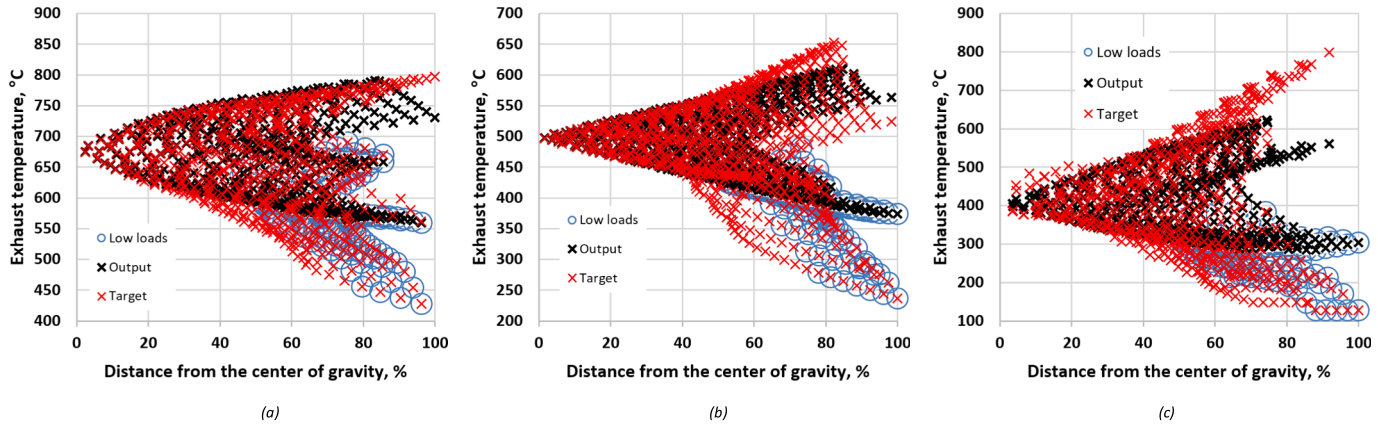

Fig. 17. Comparison between the target and expected exhaust temperature for the three datasets: LD-SI *(a)*, HD-SI *(b)* and LD-CI *(c)*.

SOI for the CI one, in comparison with the ECU data (target). The combustion timing parameter is described with great precision for SI engines, except in some areas where very different strategies prevail compared to the one predominant in the training zone. Instead, for the CI, there are some notable differences in almost all the operating plane since for this kind of engine, SOI has a more complex dependence on operating conditions. The calibration of the ECU, in different areas of the engine map, will be reflected in different correlations between the inputs and outputs of the network. Therefore, the network, trained in a limited area of the engine map, will make larger prediction errors in other areas of the map. This is because, unlike the engine torque case, the type of nonlinear link between the input and output of the network strongly changes from the training area to the prediction area, due to different control strategies, while the network predictions tend to follow the links learned with the strategies implemented in the training area. For example, with reference to a SI engine, the ECU could set a high spark advance for best fuel consumption at medium loads and a low SA for lower NOx emission at high loads. The case of the compression ignition engine is more complex because the control unit could modify the SOI also by modifying the number of diesel injections or the dwell time

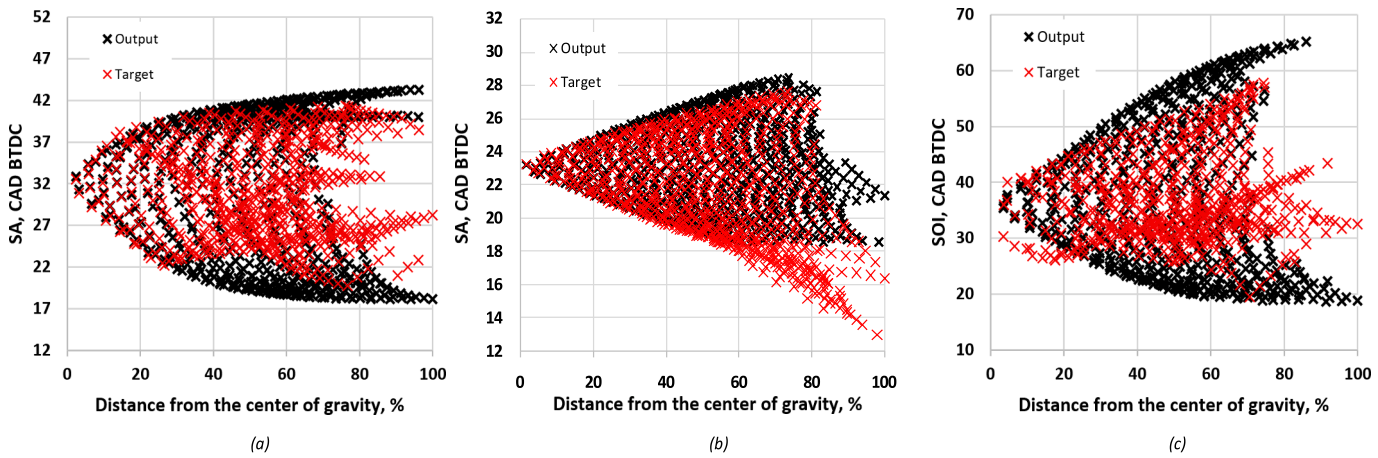

Fig. 18. Comparison between the target and expected combustion-timing parameter for the three datasets: LD-SI *(a)*, HD-SI *(b)* and LD-CI *(c)*.

between injections. Fig. 19 shows the second governing parameter related to the load: fuel flow rate for SI and MAP for the CI. In this case too, SI predictions, especially for HD-SI one, are better in comparison with CI ones. This because the stoichiometric SI cases are simpler to model, since the fuel flow rate, set by the ECU just acting on the injection time, is strictly related to the MAP, which is an input of the MLP. Instead, the worst forecast of the two governing parameters for the CI engine is due to the more complexity, as demonstrated by the higher MAPE value, already in the training. The MAP, achieved by the ECU changing the air boost level, is not simply related to the fuel flow rate, which is an input to the MLP model, but depends on how the fuel flow rate is set. Actually, the ECU sets the fuel flow rate acting not only on the injection time, as in the case of a SI engine but also on the injection pressure and with different injection splits. Therefore, the use of the only fuel flow rate as input to the MLP implies that not all the parameters influencing the real MAP were considered in the model, which therefore calculates a less accurate value. This choice was knowingly made with the objective to establish a simple and sufficiently reliable method to find first-attempt control maps to be further refined with targeted and limited experimental activity.

3.1. Comparison with a best fitting method

Since the prediction of the MLP model is central to the proposed procedure, a comparison was made with a simple model of the best fitting surfaces, as this is also a first approximation method widely used to make predictions without particular computational efforts. The easy-to-apply best fitting method, consists in the definition of the most accurate interpolation surface in two dimensions. Therefore, an interpolating surface was determined for each output of Fig. 7. Obviously, the same as the MLP model have been considered input variables: rpm / MAP for SI engines and rpm / FUEL for CI engines. The comparison between the MLP model and the best fitting method was performed in two ways. In a case, the optimal best fitting function was researched only on the basis of the data available in the range 0–20%. In the other case, the full 0–100% data set was considered to select the best fitting function, then the function calibration parameter was defined using only the data available in the range 0–20%. The two functions were chosen from a database of about 300 functions, with 3 and 4 calibration parameters, by using a dedicated software that selects the best results through the comparison of the reduced chi-squared values of the fits [23]. The method of choosing the best fitting function, based only on the data available in the 0–20% training area, is the correct operating mode for the comparison with the MLP model used in this paper, since only in this restricted area the MLP model has been trained. In contrast, the mode of selecting a function compatible with the entire definition domain (0–100%) would not be an operating mode that can be pursued in a real application, where only data in a restricted range are available, since the trend of the surface outside the training domain is not known a priori. Nevertheless, this last case can be regarded as the one in which at least a qualitative trend of the data is known from similar applications.

Fig. 20 shows the comparison between the predictions obtained using both best fitting models with those of the proposed neural network model. The first result is that the comparison can strongly depend on the characteristics of the analyzed system. In fact, for the HD engine, characterized by a small range of engine speed, slightly better

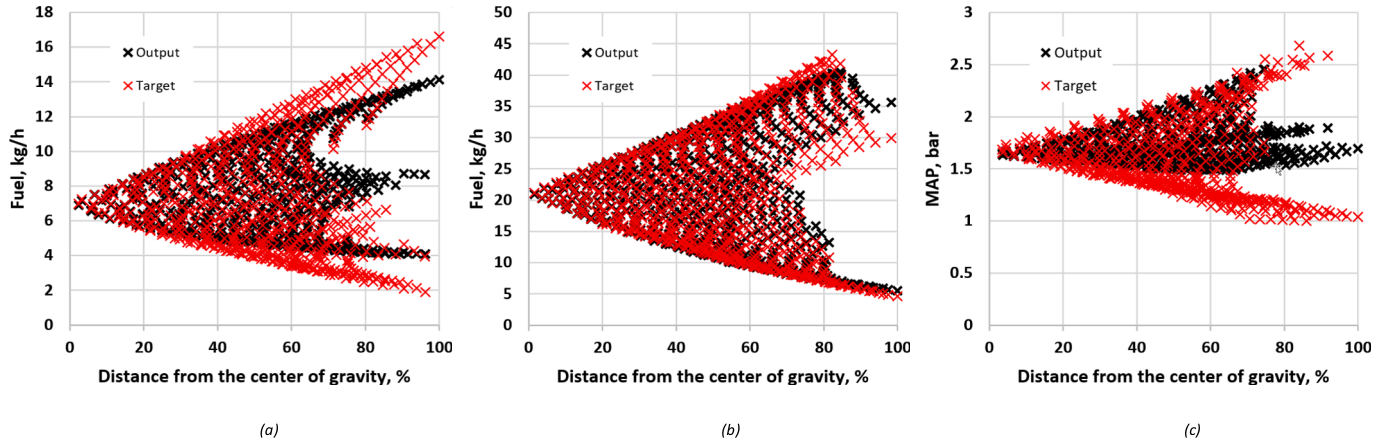

Fig. 19. Comparison between the target and expected load-control parameter for the three datasets: LD-SI *(a)*, HD-SI *(b)* and LD-CI *(c)*.

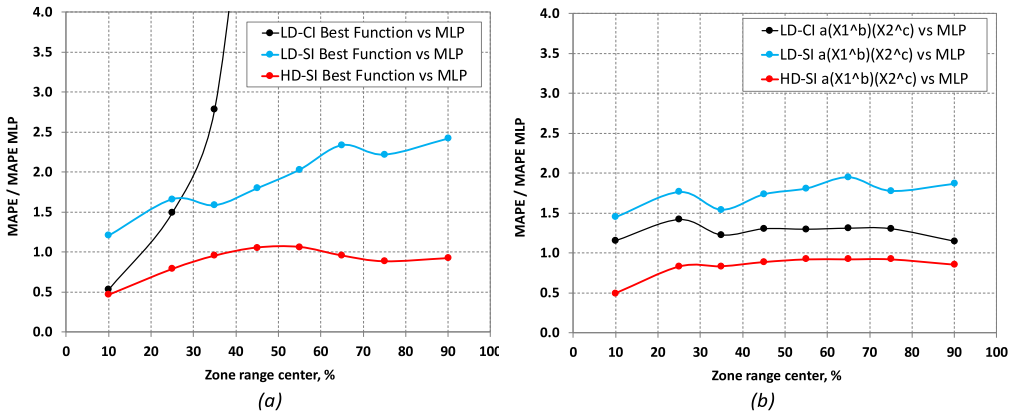

Fig. 20. Comparison between the MLP model and the models with best fitting surfaces: case of using only the data in the training area to identify the best fitting curves *(a)*, calibration case, with only the data in the training area, of a function that closely approximates the entire domain of definition *(b)*.

predictions were obtained for both best fitting models than the MLP model, over the entire definition domain. In contrast, for the two LD engines, with a wider range of engine speed, the predictions with the best fitting models can be significantly off target compared to those of the MLP model. In particular, the best fitting model approaches the MLP model only in the training zone, while deviates a lot from the real data in the forecast zone, especially for the LD-CI engine, Fig. 20a. Only by exploiting the knowledge of the qualitative trend of the data in the entire definition domain, it is possible to obtain forecasts not strongly divergent with the best fitting surface model for the two light-duty engines, besides the HD one, Fig. 20b. Therefore, the HD engine is to be considered as a particular case in which the fitting curves, identified in the 0–20% zone, are sufficiently approximated even in the 20–100% zone. This eventuality is probably due to the engine behavior, for which there is a reduced variation in speed between the training zone and the forecast zone. Therefore, the MLP model is to be considered the most reliable, resulting in a halving of the forecast error, compared to the most positive case of the best fitting method. For this last, in addition to the data in the range 0–20%, a qualitative trend of the data in the whole prediction domain is known, an aspect not always available and not used in the MLP model.

4. Conclusions

The growing complexity of new propulsion systems and driving assistance strategies makes, in the absence of reliable mathematical models, the number of experimental tests required for control calibration ever higher. With the aim of developing a simple framework, to calibrate control maps for propulsion systems with fewer experimental tests, an analysis of three engine datasets has been carried out using MLP-ANN trained in a confined portion of the whole operating map. The trained network was used to predict optimal values of control parameters and engine performance outside the calibration area, for extrapolating the experimental optimization performed in the training zone.

The model predicts the maximum engine torque with high accuracy for the cases under study, despite full torque falls within the forecast area and far from the training set. Instead, parameters much related to control strategies or physical phenomena, irrelevant in the training zone, are affected by forecasting discrepancies. However, the global behavior of the engine results sufficiently well captured by the model. The results show the possibility of using the model, defined on a barycentric portion that covered about a 10% of the engine-operating plan, to expand the area with optimal control parameters by 200%, with an error of approximately 5 times that of the training phase. This allows the use of the proposed framework to define the optimal first-attempt values, for the control parameters in not-explored system map, to be experimentally tested and refined, using the data predicted by the model. However, it is crucial to obtain very reliable data in the training area of the operating plan, to achieve a relatively low MAPE. Indeed, in the forecast region, the MAPE was found to grow roughly according to an exponential fitting with the distance from the training zone. The used forecasting method was compared with another simple alternative one, the best fitting surfaces, resulting considerably more reliable with an average prediction error at least more than halved in the areas farthest from the training.

CRediT authorship contribution statement

Luigi De Simio: Conceptualization, Methodology, Software, Writing – review & editing. **Sabato Iannaccone:** Conceptualization, Writing – review & editing. **Aniello Iazzetta:** Data curation, Software. **Maddalena Auriemma:** Writing – review & editing.

Declaration of Competing Interest

The authors declare that they have no known competing financial interests or personal relationships that could have appeared to influence the work reported in this paper.

Data availability

Data will be made available on request.

Acknowledgments

The authors would like to thank Vincenzo Bonanno for his valuable support in experimental activities.

References

[1] Gu F, Jacob PJ, Ball AD. (1996). A RBF neural network model for cylinder pressure reconstruction in internal combustion engines. *IEE Colloq. Model. Signal Process. Fault Diagnosis* (Digest No 1996260), 4:1–411. 10.1049ic19961374.
[2] Bizon K, Continillo G, Lombardi S, Mancaruso E, Maria VB. ANN-based virtual sensor for on-line prediction of in-cylinder pressure in a diesel engine. Comput Aided Chem Eng 2014;33:763–8. https://doi.org/10.1016/B978-0-444-63456-6.50128-9.
[3] Hoffmann K, Seebach D, Pischinger S, Abel D. Neural networks for controlling and modelling future low temperature combustion technologies. IFAC Proc 2007;2007 (40):19–24. https://doi.org/10.3182/20071029-2-FR-4913.00005.
[4] Liu J, Huang Q, Ulishney C, Dumitrescu CE. Machine learning assisted prediction of exhaust gas temperature of a heavy-duty natural gas spark ignition engine. Appl Energy 2021;300:117413. https://doi.org/10.1016/j.apenergy.2021.117413.
[5] Che Wan MN, Mamat R, Ahmed A. (2018). Comparative Study of Artificial Neural Network and Mathematical Model on Marine Diesel Engine Performance Prediction. *Int J Innov Comput Inf Control IJICIC*, 14. http://www.ijicic.org/ijicic-140313.pdf.
[6] Serikov SA. Neural network model of internal combustion engine. Cybern Syst Anal 2010;46:998–1007. https://doi.org/10.1007/s10559-010-9281-3.

[7] Mart JD. Modeling of internal combustion engine emissions by LOLIMOT algorithm. Procedia Technol 2012;3:251–8. https://doi.org/10.1016/j.protcy.2012.03.027.
[8] Özener O, Yüksek L, Özkan M. Artificial neural network approach to predicting engine-out emissions and performance parameters of a turbo charged diesel engine. Therm Sci 2013;17:153–66. https://doi.org/10.2298/TSCI120321220O.
[9] Jahirul MI, Rahman S, Masjuki HH, Kalam MA, Rashid M. Application of artificial neural networks for prediction the performance of a dual fuel internal combustion engine. HKIE Trans Hong Kong Inst Eng 2009;16:14–20. https://doi.org/10.1080/1023697X.2009.10668146.
[10] Boruah D, Thakur PK DB. (2016). Artificial neural network based modelling of internal Combustion Engine Performance. *IJERT*, 5:568–76. 10.17577/IJERTV5IS030924.
[11] Nwufo OC, Okwu M, Nwaiwu CF, Igbokwe JO, Nwafor OMI, Anyanwu EE. The Application of Artificial Neural Network in Prediction of the Performance of Spark Ignition Engine Running on Ethanol-Petrol Blends. Adv Mech Eng 2017;12:15–31.
[12] Uslu S, Celik MB. Prediction of engine emissions and performance with artificial neural networks in a single cylinder diesel engine using diethyl ether. Eng Sci Technol an Int J 2018;21:1194–201. https://doi.org/10.1016/j.jestch.2018.08.017.
[13] Liu Z, Zuo Q, Wu G, Li Y. An artificial neural network developed for predicting of performance and emissions of a spark ignition engine fueled with butanol – gasoline blends. Adv Mech Eng 2018;10:1–11. https://doi.org/10.1177/1687814017748438.
[14] Yusri IM, Majeed APPA, Mamat R, Ghazali MF, Awad OI, Azmi WH. A review on the application of response surface method and artificial neural network in engine performance and exhaust emissions characteristics in alternative fuel. Renew Sustain Energy Rev 2018;90:665–86. https://doi.org/10.1016/j.rser.2018.03.095.
[15] Gumus K, Sen A. (2013). Comparison of spatial interpolation methods and multi-layer neural networks for different point distributions on a digital elevation model. *Geod Vestn*, 57:523–43. 10.15292/geodetski-vestnik.2013.03.523-543.
[16] Turkson RF, Yan F, Aliet MKA, Hu J. Artificial neural network applications in the calibration of spark-ignition engines: An overview. Eng Sci Tech Int J 2016;19:1346–59. https://doi.org/10.1016/j.jestch.2016.03.003.
[17] Cybenko G. Approximation by superpositions of a sigmoidal function. Math Control Signal Syst 1989;2:303–14. https://doi.org/10.1007/BF02551274.
[18] Raza K, Jothiprakash V. Multi-output ANN Model for Prediction of Seven Meteorological Parameters in a Weather Station. J Inst Eng India Ser A 2014;95:221–9. https://doi.org/10.1007/s40030-014-0092-9.
[19] Pandey DS, Das S, Pan I, Leahy J, Kwapinski W. Artificial neural network based modelling approach for municipal solid waste gasification in a fluidized bed reactor. Waste Manag 2016;58:202–13. https://doi.org/10.1016/j.wasman.2016.08.023.
[20] Bhatt AN, Shrivastava N. Application of Artificial Neural Network for Internal Combustion Engines: A State of the Art Review. Arch Computat Methods Eng 2022;29:897–919. https://doi.org/10.1007/s11831-021-09596-5.
[21] Ding S, Li H, Su C, Yu J, Jin F. Evolutionary artificial neural networks: a review. Artif Intell Rev 2013;39:251–60. https://doi.org/10.1007/s10462-011-9270-6.
[22] De Falco I, Della Cioppa A, Iazzetta A, Tarantino E. (1998). MijnMutation Operator for Aerofoil Design Optimisation. In: Chawdhry PK, Roy R, Pant RK, editors. *Soft Comput. Eng. Des. Manuf.*, London: Springer London, 211–20. 10.1007/978-1-4471-0427-8_23.
[23] Silva W.P. and Silva C.M.D.P.S., LAB Fit Curve Fitting Software (Nonlinear Regression and Treatment of Data Program) V 7.2.50c (1999-2022), online, available from world wide web: www.labfit.net. Accessed April 10, 2022.